Cell Death and Differentiation (2015) 22, 1654–1664

www.nature.com/cdd

Osteoblast-induced osteoclast apoptosis by fas ligand/FAS pathway is required for maintenance of bone mass

L Wang[1,2,6], S Liu[1,3,6], Y Zhao[1], D Liu[4], Y Liu[4], C Chen[4], S Karray[5], S Shi*[,1,3,4] and Y Jin*[,1,3]

The interplay between osteoblasts and osteoclasts has a crucial role in maintaining bone homeostasis. In this study, we reveal that osteoblasts are capable of inducing osteoclast apoptosis by FAS ligand (FASL)/FAS signaling. Conditional knockout of FASL in osteoblasts results in elevated osteoclast numbers and activity, along with reduced bone mass, suggesting that osteoblast-produced FASL is required to maintain physiological bone mass. More interestingly, we show that osteoblasts from ovariectomized (OVX) osteoporotic mice exhibit decreased FASL expression that results from the IFN-γ- and TNF-α-activated NF-κB pathway, leading to reduced osteoclast apoptosis and increased bone resorption. Systemic administration of either IFN-γ or TNF-α ameliorates the osteoporotic phenotype in OVX mice and rescues FASL expression in osteoblasts. In addition, ovariectomy induces more significant bone loss in FASL conditional knockout mice than in control group with increased osteoclast activity in which the levels of RANKL and OPG remain unchanged. Taken together, this study suggests that osteoblast-induced osteoclast apoptosis via FASL/FAS signaling is a previously unrecognized mechanism that has an important role in the maintenance of bone mass in both physiological conditions and OVX osteoporosis.
Cell Death and Differentiation (2015) **22,** 1654–1664; doi:10.1038/cdd.2015.14; published online 6 March 2015

A delicate balance between osteoclastic and osteoblastic activities is required to maintain bone homeostasis. Bone-resorbing osteoclasts are multinucleated cells derived from monocyte-macrophage precursors with haematopoietic stem cell (HSC) origin, whereas bone-forming osteoblasts are derived from mesenchymal stem cells (MSC). It has been demonstrated that osteoblasts maintain the stem cell niche of HSCs, regulate their differentiation and are capable of inducing HSC-derived T-cell apoptosis.[1–4] On the other hand, T cells can impair osteoblast progenitors by secreting proinflammatory cytokines such as IFN-γ and TNF-α.[5,6] Several signaling pathways have been identified as contributing to the interplay between osteoblasts and osteoclasts, including receptor activator of NF-κB (RANK) and its ligand RANKL, EphrinB2/EphB4, Sema4D and Sema3A.[7–10] Of these, RANKL/OPG is the best-established regulatory mechanism controlling osteoclast development and function.[11] Osteoblast lineage cells produce RANKL and stimulate their RANK receptors on osteoclast precursors, resulting in osteoclast differentiation by activating the downstream signaling pathway transcription factors NF-κB, c-FOS and NFATc1 (nuclear factor of activated T cells c1).[10,12–16] Osteoblasts also produce osteoprotegerin (OPG), a decoy receptor for RANKL, to balance osteoclastogenesis *in vivo*.[17] However, it is unknown whether direct contact between osteoblasts and osteoclasts also regulates their interplay in physiological conditions to maintain bone mass.

FAS ligand (FASL or CD95L) is a transmembrane protein that belongs to the TNF family. Its binding with FAS receptor represents an important apoptotic signal in many cell types, thereby regulating the immune system and the progression of cancer.[18–20] Decreased apoptosis in osteoclasts has been suggested as one of the causes of osteoporosis.[21,22] Recent study showed that estrogen may elevate FASL expression in osteoblasts, leading to osteoblast-mediated apoptosis of osteoclast progenitors.[23] Such paracrine signaling was further identified in the regulation of MMP3-induced FASL cleavage in osteoblasts by ERα, resulting in the secretion of soluble FASL (sFASL) and the induction of osteoclast apoptosis.[24] These studies provided experimental evidence that the bone-protective effect of estrogen against osteoporosis may derive, at least partially, from the interplay between osteoblasts and

[1]State Key Laboratory of Military Stomatology, Center for Tissue Engineering, School of Stomatology, The Fourth Military Medical University, Xi'an, Shaanxi 710032, China; [2]State Key Laboratory of Military Stomatology, Department of Oral and Maxillofacial Surgery, School of Stomatology, The Fourth Military Medical University, Xi'an, Shaanxi 710032, China; [3]Research and Development Center for Tissue Engineering, The Fourth Military Medical University, Xi'an, Shaanxi 710032, China; [4]Department of Anatomy and Cell Biology, School of Dental Medicine, University of Pennsylvania, Philadelphia, PA, USA and [5]INSERM U753, Institut Gustave Roussy, Villejuif Cedex, France
*Corresponding author: Y Jin, State Key Laboratory of Military Stomatology, Center for Tissue Engineering, School of Stomatology, The Fourth Military Medical University, 145 West Changle Road, Xi'an, Shaanxi 710032, China. Tel: +86 29 8477 6147; Fax: +86 29 8321 8039; E-mail: yanjinfmmu@vip.sina.com
or S Shi, Department of Anatomy and Cell Biology, School of Dental Medicine, University of Pennsylvania, Philadelphia, PA, USA. Tel: +1 240 793 0641; Fax: +1 215 573 2324; E-mail: songtaos@dental.upenn.edu
[6]These authors contributed equally to this work.

Abbreviations: FASL, FAS ligand; OVX, ovariectomized; HSC, haematopoietic stem cell; MSC, mesenchymal stem cells; RANK, receptor activator of NF-κB; RANKL, receptor activator of NF-κB ligand; NFATc1, nuclear factor of activated T cells c1; OPG, osteoprotegerin; sFASL, soluble FASL; cKO, conditional knockout; BMD, bone mineral density; BV/TV, bone volume/total volume; μCT, micro-CT; N. Oc/BS, number of osteoclasts/bone surface; Oc. S/BS, osteoclast surface/bone surface ratio; BMMs, bone marrow-derived monocyte/macrophage precursor cells; M-CSF, macrophage colony-stimulating factor; TUNEL, terminal deoxynucleotidyl transferase dUTP nick end labeling; TRAP, tartrate-resistant acid phosphatase; Ob. S/BS, osteoblast surface/bone surface ratio; HA/TCP, hydroxyapatite/tricalcium phosphate; PBMNCs, peripheral blood mononuclear cells; CCR2, C-C chemokine receptor-2; PFA, paraformaldehyde; BMCs, bone marrow cells

Received 29.10.14; revised 05.1.15; accepted 19.1.15; Edited by J Silke; published online 06.3.15

osteoclasts. However, the detailed functional role that FASL has in osteoblasts to regulate the pathophysiology of osteoporosis is unknown. Therefore, in addition to the RANKL/OPG system, we show in this study that osteoblasts govern bone mass in both physiological conditions and osteoporosis by inducing osteoclast apoptosis via the FASL/FAS pathway in a paracrine manner.

Results

FASL conditional knockout (cKO) mice show osteopenic phenotype and decreased osteoclast apoptosis. To evaluate whether FASL expression in the osteoblast lineage cells has any effect on the maintenance of bone mass *in vivo*, we generated osteoblast progenitor/osteoblast-specific FASL-deficient mice (FASL cKO) by crossing animals bearing conditional FASL knockout alleles ($FASL^{fl/fl}$)[25,26] to transgenic mice expressing Cre recombinase gene under the SP7 promoter (B6.Cg-Tg(Sp7-tTA,tetO-EGFP/cre)1Amc/J),[27] in which the Cre is inserted into the *FASl* locus and specifically expressed in the osteoblastic lineage (Supplementary Figure 1A). The FASL cKO mice were born alive and at predicted Mendelian frequencies, with no apparent skeletal morphological abnormalities at birth (Supplementary Figure 1B). With specific expression of Cre in bone tissue, FASL was essentially undetectable in osteoblasts derived from adult FASL cKO mice (Supplementary Figure 1C), whereas FASL expression in other tissues was comparable to the levels found in $FASL^{fl/fl}$ mice (data not shown), indicating a nearly complete ablation of FASL expression in the osteoblast lineage. However, adult FASL cKO mice exhibited an osteopenic phenotype, whereas control littermates ($FASL^{fl/fl}$) did not, and markedly reduced bone mineral density (BMD) and bone volume/total volume (BV/TV) in the femurs, as assessed by micro-CT (μCT) analysis (Figure 1a). H&E and *von* Kossa staining showed a reduced bone trabeculae percentage in the femurs of FASL cKO mice (Figure 1b). Histomorphometric analyses revealed that the femur bone trabeculae percentage in FASL cKO mice was markedly lower than in control littermates (Figure 1b). Notably, TRAP staining showed that FASL cKO mice had a markedly elevated number of osteoclasts/bone surface (N. Oc/BS) and increased osteoclast surface/bone surface ratio (Oc. S/BS) (Figure 1c). Terminal deoxynucleotidyl transferase dUTP nick end labeling (TUNEL)-tartrate-resistant acid phosphatase (TRAP) double staining revealed that FASL cKO mice presented a markedly reduced number of $TUNEL^{+}TRAP^{+}$ apoptotic osteoclasts compared with control littermates, suggesting that the activated osteoclast activity could be attributed, at least in part, to the reduced osteoclast apoptosis (Figure 1d). Using an *in vivo* osteoclast activity assay, we confirmed that the implantation of titanium particles was able to induce more bone resorption in the calvarial bones of FASL cKO mice than in control littermates (Figure 1e).

Osteoblasts are capable of inducing osteoclast apoptosis via FASL/FAS pathway to maintain bone mass. As osteoblast lineage cells express membrane-bound FASL[28]

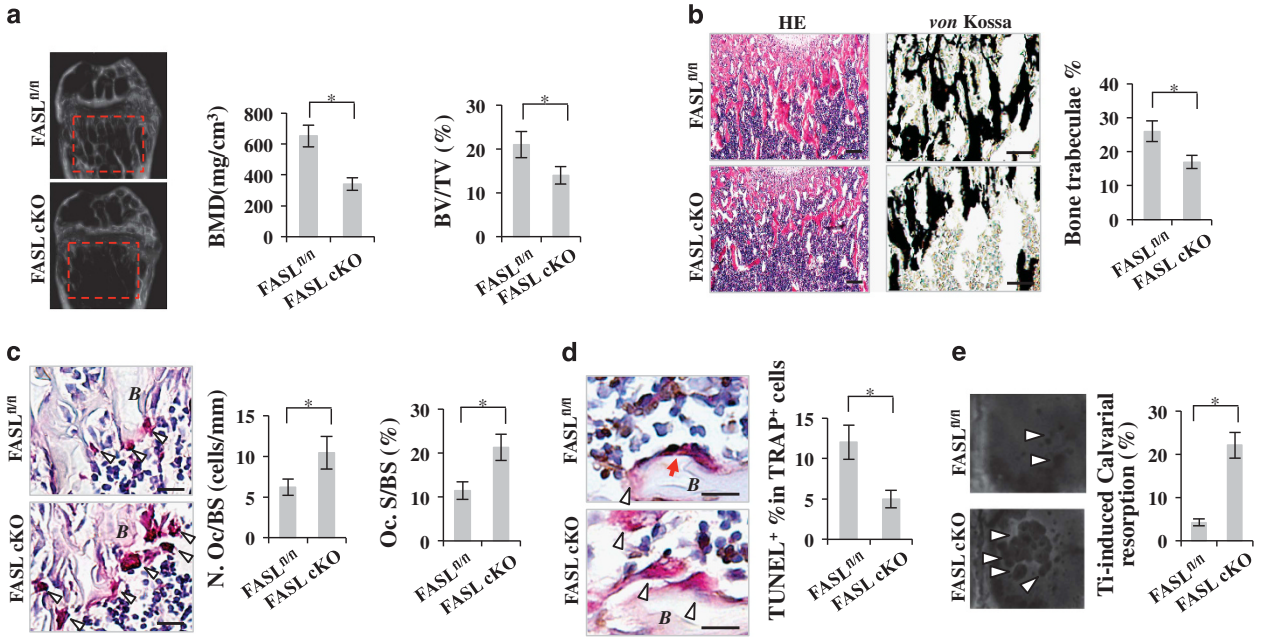

Figure 1 FASL cKO mice show osteopenic phenotype and decreased osteoclast apoptosis. (**a**) μCT analysis showed markedly reduced BMD and BV/TV in femurs of adult FASL cKO mice when compared with the control littermates ($FASL^{fl/fl}$). (**b**) H&E and von Kossa staining showed reduced bone trabeculae in the femurs of FASL cKO mice, and histomorphometric analyses revealed that bone trabeculae percentage in FASL cKO mice were markedly lower than those metrics as measured in control littermates. (**c**) TRAP staining showed that FASL cKO mice exhibited an increased number of osteoclasts/bone surface (N. Oc/BS) and osteoclast surface/bone surface ratio (Oc. S/BS). (**d**) TUNEL-TRAP double staining showed that FASL cKO mice presented a significantly reduced number of $TUNEL^{+}TRAP^{+}$ apoptotic osteoclasts compared with the control littermates. (**e**) Using an *in vivo* titanium particles implantation assay, we showed that titanium particles induced more bone resorption in calvarial bones of FASL cKO mice than observed in control littermates. B, bone; Red arrows, apoptotic nuclear; white triangles, $TRAP^{+}$ cells in **c** and **d** and bone resorption pits in **e**; Error bars represent mean $\pm$ S.E.M., $n=8$ animals per group, and all the experiments were performed in triplicate. $^{*}P<0.05$. Scale bar, 100 μm

and have a high chance of contact with FAS-positive osteoclasts during the bone remodeling process,[21,29] we hypothesized that osteoblast lineage cells might be capable of inducing osteoclast apoptosis via membrane-bound FASL to maintain bone mass. To test this hypothesis, we cocultured osteoblasts from C57BL6 mice (WT Obs), FASL-mutated B6Smn.C3-FASL*gld*/J mice (FASL-null Obs) and FASL-transfected FASL-null osteoblasts (FASL$^+$/FASL-null Obs), respectively, with matured osteoclasts. The osteoclasts were differentiated from bone marrow-derived monocyte/macrophage precursor cells (BMMs) stimulated by RANKL and macrophage colony-stimulating factor (M-CSF, Figure 2a). We observed marked osteoclast apoptosis in the WT osteoblast and FASL$^+$/FASL-null osteoblast groups, but not in the FASL-null osteoblast group, as determined by TUNEL-TRAP double staining (Figure 2a), suggesting that osteoblast-produced FASL can directly induce osteoclast apoptosis. We also found that FASL expression of osteoblast lineage cells decreased during their differentiation from osteoblast progenitors to mature osteoblast (Supplementary Figure 2A). When osteoblasts and osteoclasts were cocultured in a transwell system, no marked osteoclast apoptosis was observed (Figure 2b), suggesting that cell–cell contact is required for the induction of osteoclast apoptosis by osteoblasts. To confirm that FAS receptor is further required for the induction of osteoclast apoptosis by osteoblasts, we demonstrated that WT osteoblasts were not able to induce apoptosis in mature osteoclasts derived from FAS-mutated C3MRLFAS *lpr*/J mice (FAS-null osteoclasts), whereas FAS-transfected FAS-null osteoclasts (FAS$^+$/FAS-null osteoclasts) showed marked apoptosis when cocultured with WT osteoblasts (Figure 2c). This confirms that the FASL/FAS pathway is required for osteoblast-induced osteoclast apoptosis *in vitro*. We also found that, compared with mature osteoclasts, osteoclast progenitors had lower FAS expression and showed much lower sensitivity to osteoblast-induced apoptosis (Supplementary Figures 2B–D). Moreover, we demonstrated that osteoblasts derived from FASL cKO mice showed markedly decreased capacity to induce osteoclast apoptosis compared with osteoblasts from control

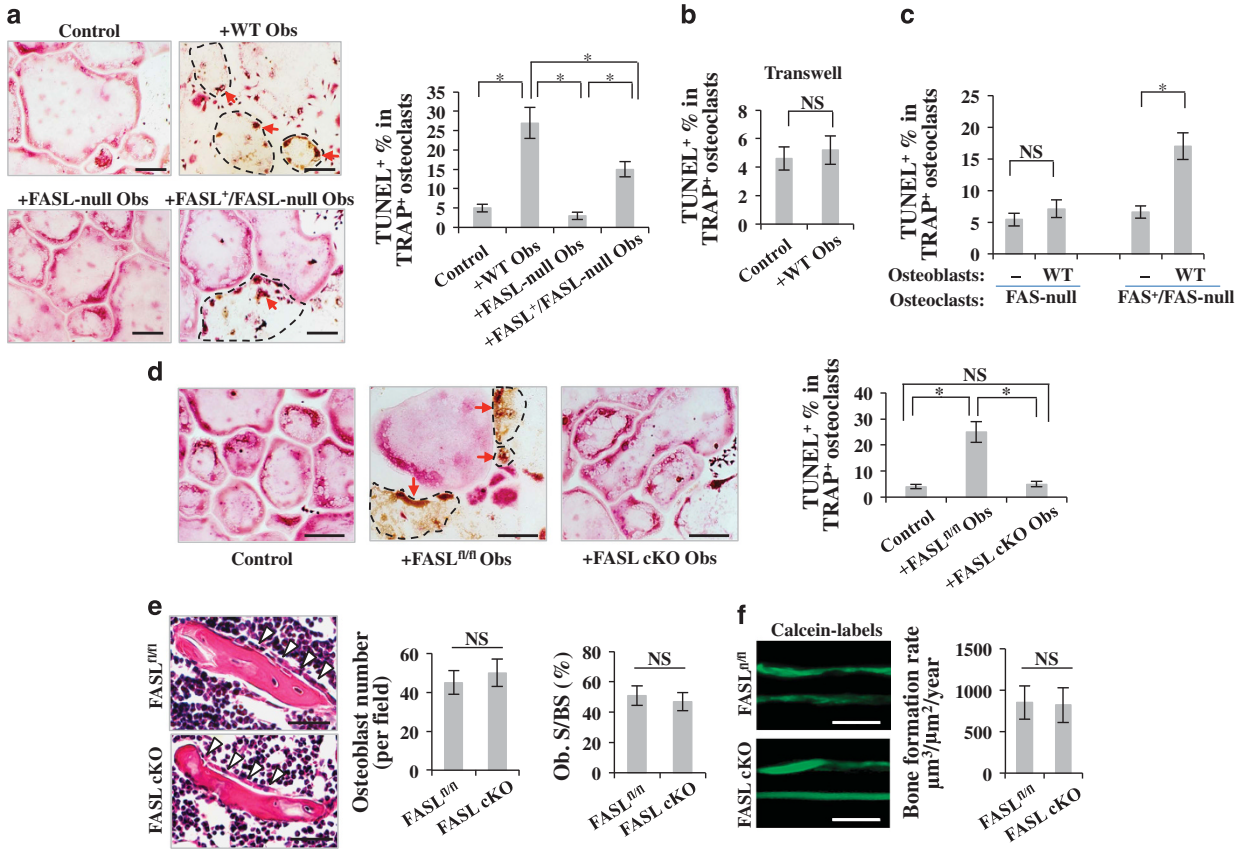

Figure 2 Osteoblasts are capable of inducing osteoclast apoptosis via FASL/FAS pathway. (**a**) After coculture of osteoblasts from C57BL6 mice (WT Obs), FASL-mutated B6Smn.C3- FASLgld/J mice (FASL-null Obs) and FASL-transfected FASL-null osteoblasts (FASL$^+$/FASL-null Obs) with matured osteoclasts, TUNEL-TRAP double staining showed a marked osteoclast apoptosis induced by WT Obs and FASL$^+$/FASL-null Obs, but not FASL-null Obs. (**b**) When osteoblasts and osteoclasts were cocultured in a transwell system, no marked osteoclast apoptosis was observed. (**c**) When cocultured with osteoclasts from FAS-mutated C3MRLFAS *lpr*/J mice (FAS-null osteoclasts), WT osteoblasts failed to induce matured osteoclast apoptosis, whereas WT osteoblasts were able to induce FAS-transfected FAS-null osteoclast (FAS$^+$/FAS-null osteoclasts) apoptosis in the coculture system. (**d**) TUNEL-TRAP double staining showed that osteoblasts derived from FASL cKO mice exhibited decreased capacity to induce osteoclast apoptosis compared with those from the control littermates when cocultured with matured WT osteoclasts. (**e**) H&E staining showed no significant difference in osteoblast number per field and osteoblast surface/bone surface ratio (Ob. S/BS) in the femurs between FASL cKO mice and the control littermates. (**f**) Calcein labeling showed no significant difference in the amount of newly formed bone between FASL cKO mice and the control littermates. Dashed lines, TUNEL$^-$TRAP$^+$ cells; red arrows, apoptotic nuclears; error bars represent mean $\pm$ S.E.M., and all the experiments were performed in triplicate, $n=8$ animals per group. *$P<0.05$. Scale bar, 100 μm

littermates, when cocultured with matured WT osteoclasts (Figure 2d). To confirm that mature osteoblasts from mouse calvarial bones show similar effects in terms of inducing osteoclast apoptosis, we cocultured calvarial osteoblasts with mature osteoclasts, and we also observed a substantial amount of osteoclast apoptosis (data not shown).

To determine whether the osteopenic phenotype in FASL cKO mice was attributable to osteoblast number and function, we performed static histomorphometric analysis of the number of osteoblasts, osteoblast surface/bone surface ratio (Ob. S/BS) and osteoid thickness, in addition to a calcein-labeling assay, but we failed to detect any significant difference between FASL cKO mice and their control littermates (Figures 2e and f,Supplementary Figure 3A). We further revealed that osteoblast progenitors derived from FASL cKO mice had the same capacity for osteogenic differentiation as those of control littermates, as indicated by Alizarin Red staining to show increased mineralized nodule formation *in vitro*. We also implanted osteoblast progenitors subcutaneously into immunocompromised mice using hydroxyapatite/tricalcium phosphate (HA/TCP) as a carrier to evaluate *in vivo* bone formation (Supplementary Figures 3B and D). In addition, osteoblast progenitors derived from FASL cKO mice were compared with ones from control littermates and found to have equivalent self-renewal capacities, proliferation rates and adipogenesis differentiation potentials, as determined by population-doubling analysis, BrdU incorporation assay and Oil Red staining, respectively (Supplementary Figures 3E and G). These data suggest that osteoblast progenitors from FASL cKO mice show reduced capability to induce osteoclast apoptosis, but nevertheless retain normal bone-forming capacity.

To determine whether osteoclast differentiation is altered in FASL cKO mice, we performed flow cytometric analysis of $CD11b^{low/-}CD3\varepsilon^{-}B220^{-}c\text{-}Kit^{+}c\text{-}Fms^{+}$ cells and immunostaining of RANK in bone marrow.[30] We found no significant difference in the number of osteoclast progenitors between FASL cKO mice and control littermates (Supplementary Figures 4A and B). Although FASL cKO mice exhibit markedly elevated numbers of osteoclasts, bone marrow cells from FASL cKO mice showed a normal capacity to generate osteoclasts in response to the induction of either M-CSF alone or M-CSF and RANKL in combination (Supplementary Figure 4C). In addition, western blot analysis showed that the level of FAS expression in osteoclasts of FASL cKO mice was similar to that of control littermates (Supplementary Figure 4D), suggesting that osteoclast apoptosis in FASL cKO mice does not result from the elevation of FAS expression in osteoclasts. Moreover, after coculture with WT osteoblasts, osteoclasts derived from FASL cKO mice showed a rate of apoptosis equivalent to the rate seen in control littermates (Supplementary Figure 4E). Taken together, these data suggest that specific knockdown of FASL in osteoblastic cells fails to affect osteoclastogenesis. As osteoblastic cells maintain the stem cell niche of HSCs,[1–4] we next investigated whether there was a difference in the number of HSCs between FASL cKO mice and their control littermates. No significant difference was found (Supplementary Figure 5A). Furthermore, no marked difference in the percentage of Th1, Th2, Th17 and Tregs was observed in the peripheral blood mononuclear cells (PBMNCs); serum concentrations of cytokine IFNγ, TNFα, IL17 and IL1β, white blood cell percentage and red blood cell count in the peripheral blood were all comparable in FASL cKO mice and control littermates (Supplementary Figures 5B and E). Additional evidence in support of our hypothesis includes our findings that FASL-null *gld* mice also showed decreased BMD and trabecular bone structures, an elevated number of osteoclasts, a decreased number of $TUNEL^{+}TRAP^{+}$ apoptotic osteoclasts and increased bone resorption in the calvarial bones following the implantation of titanium particles when compared with control littermates (Supplementary Figures 6A and E).

Blockage of RANKL shows limited ability to rescue the osteopenic phenotype in FASL cKO mice. As RANKL is an important factor enabling osteoblastic cells to regulate osteoclast development and function,[10–16] we next examined expression levels of RANKL and OPG in FASL cKO mice, and we found no significant difference in the levels of RANKL and OPG in either serum or osteoblast progenitors between FASL cKO mice and control littermates, as determined by ELISA and western blot, respectively (Figures 3a and b). To further clarify the role of RANKL in FASL cKO mice, we systemically administered RANKL neutralizing antibody to FASL cKO mice and control littermates. After the blockage of RANKL in control mice, the osteoclast activity was substantially reduced, as determined by the minimal TRAP staining observed in their femurs, resulting in markedly increased BMD and bone trabeculae percentage (Figures 3c and f). However, RANKL neutralizing antibody showed compromised ability to reduce the osteoclast activity in FASL cKO mice, resulting in less of an increase in BMD and bone trabeculae percentage when compared with control mice (Figures 3c and f). This indicates that RANKL has a less important role than the loss of FASL-mediated osteoclast apoptosis by osteoblasts in the osteopenic phenotype in FASL cKO mice.

FASL expression is downregulated in osteoblast progenitors/osteoblasts from OVX mice. Previous reports suggest that estrogen can drive FASL expression in osteoblasts to induce osteoclast apoptosis.[23,24] Here we examined whether the FASL expression level in osteoblasts is associated with osteopenia phenotype in OVX mice. We found that osteoblast progenitors from OVX mice showed a reduced expression of FASL when compared with sham control group, as assessed by PCR array and western blot (Figures 4a and b). Moreover, TUNEL-TRAP double staining showed that OVX mice presented a reduced number of apoptotic osteoclasts in femurs compared with control sham mice (Figure 4c). To verify that reduced osteoclast apoptosis in OVX mice results from the reduction of FASL expression in osteoblasts, we cocultured osteoblast progenitors with osteoclasts and showed that OVX-derived osteoblasts, with compromised level of FASL, induced a decreased number of apoptotic osteoclasts when compared with control sham osteoblasts (Figure 4d). To further confirm the function of FASL in osteoblast progenitors/osteoblast-induced osteoclast apoptosis, we knocked down FASL expression in control sham osteoblasts by siRNA and found that FASL-knockdown

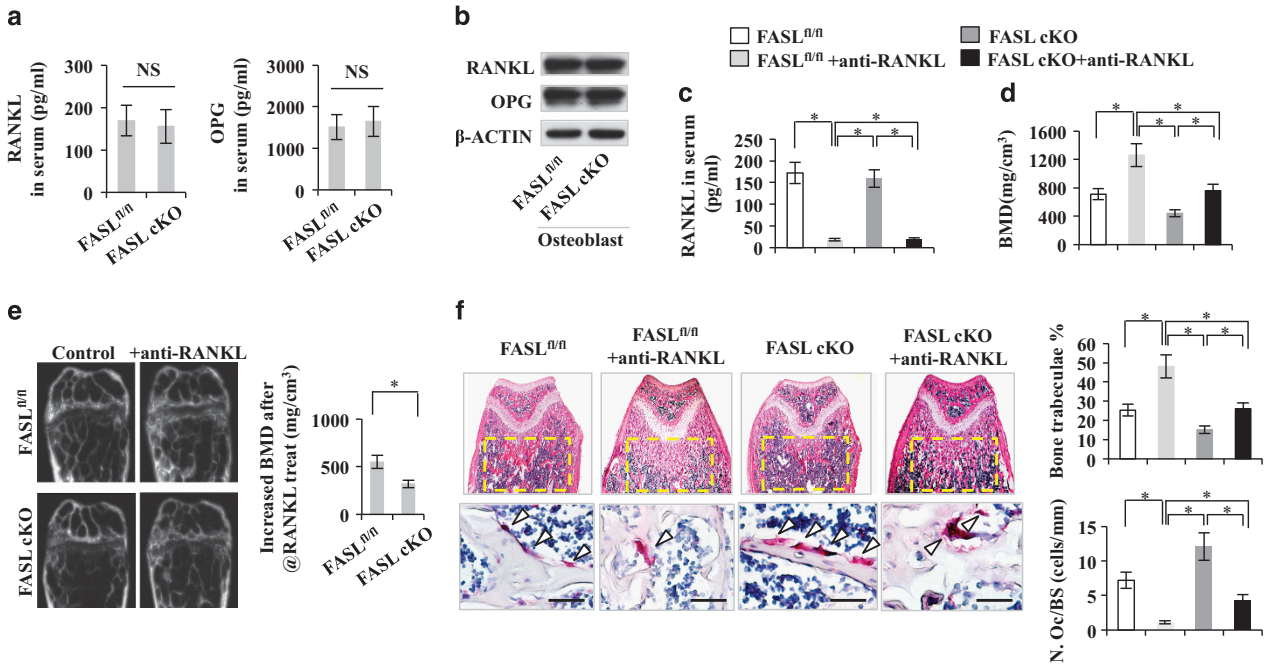

Figure 3 Blockage of RANKL shows limited ability to rescue the osteopenic phenotype in FASL cKO mice. (**a** and **b**) ELISA and western blot showed that there was no significant difference in the RANKL and OPG expression in both serum and osteoblast progenitors/osteoblast cell culture lysis of the FASL cKO mice and control littermates. (**c**) ELISA showed that RANKL neutralizing antibody was able to substantially block RANKL level in serum. (**d** and **e**) μCT showed that blockage of RANKL using its neutralizing antibody in control mice resulted in a marked increase in the BMD in femurs, whereas it showed compromised ability to increase the BMD in FASL cKO mice. (**f**) HE staining showed that blockage of RANKL in control mice resulted in a stronger ability to increase bone trabeculae percentage when compared with FASL cKO mice; TRAP staining showed that blockage of RANKL in control mice resulted in a stronger ability to reduce the osteoclast activity when compared with FASL cKO mice. White triangles, TRAP$^+$ cells; Error bars represent mean $\pm$ S.E.M., $n=6$ animals per group. *$P<0.05$. Scale bar, 100 μm

osteoblasts showed decreased capacity to induce osteoclast apoptosis (Figure 4e). On the other hand, overexpression of FASL in OVX-derived osteoblasts by lentivirus transfection resulted in increased capacity to induce osteoclast apoptosis in the coculture system (Figure 4f, Supplementary Figure 7).

As IFN-γ and TNF-α can synergistically impair osteogenic differentiation of osteoblast progenitors derived from OVX mice via the NFκB pathway,[6,31,32] we further examined whether blockage of either IFN-γ or TNF-α could rescue the FASL expression in osteoblasts of OVX mice. We found that systemic injection of either IFN-γ or TNF-α neutralizing antibody into OVX mice was able to markedly decrease the levels of IFN-γ and TNF-α, respectively, in the bone marrow (Figures 5a and b) and increase the BMD and BV/TV of femurs (Figures 5c and e). Interestingly, systemic injection of either IFN-γ or TNF-α neutralizing antibody could rescue the FASL expression with downregulation of p-IκB in the osteoblasts derived from OVX mice, and restore their capacity to induce osteoclast apoptosis *in vitro* (Figures 5f and g). Moreover, OVX failed to induce FASL downregulation in osteoblast progenitors of either IFN-γ knockout or TNF-α knockout mice (Figure 5h), suggesting that IFN-γ and TNF-α synergistically downregulate FASL expression in osteoblast progenitors. In addition, we revealed that systemic injection of NFκB inhibitor IKK Inhibitor VII was able to rescue FASL expression in OVX-derived osteoblast progenitors and restore their ability to induce osteoclast apoptosis *in vitro* (Figure 5i). To mimic such IFN-γ- and TNF-α-induced FASL downregulation, we exposed osteoblast progenitors to IFN-γ and TNF-α, either alone or in combination. Interestingly, long-term treatment of IFN-γ and TNF-α in combination, but not separately, caused the most dramatic reduction in FASL expression, along with upregulation of the NFκB pathway (Supplementary Figure 8A). IFN-γ and TNF-α treatment also resulted in a reduced ability to induce osteoclast apoptosis *in vitro,* whereas additional treatment of IKKα siRNA abolished the FASL downregulation, resulting in the rescue of osteoblast progenitor to induce osteoclast apoptosis (Supplementary Figures 8B and C).

OVX induces more dramatic bone loss in FASL cKO mice. To further confirm the osteoprotection by FASL expression in osteoblasts, we performed OVX in FASL cKO mice and their wild-type littermates, and found that FASL cKO mice showed more dramatic decreases in bone mineral density and bone trabeculae percentage in the femurs when compared with their wild-type littermates (Figures 6a and c). Notably, FASL cKO mice showed more dramatically elevated osteoclast activity as determined by TRAP staining when compared with their control littermates (Figure 6d). Although OVX was able to induce decreased ratio of apoptotic osteoclasts in wild-type mice, FASL cKO mice presented the lowest ratio of apoptotic osteoclasts regardless of sham or OVX procedures (Figure 6e), suggesting that FASL expression in osteoblasts is required to reduce the OVX-induced osteoclast activation by removing mature osteoclasts, without which the OVX-induced osteoclasts activity

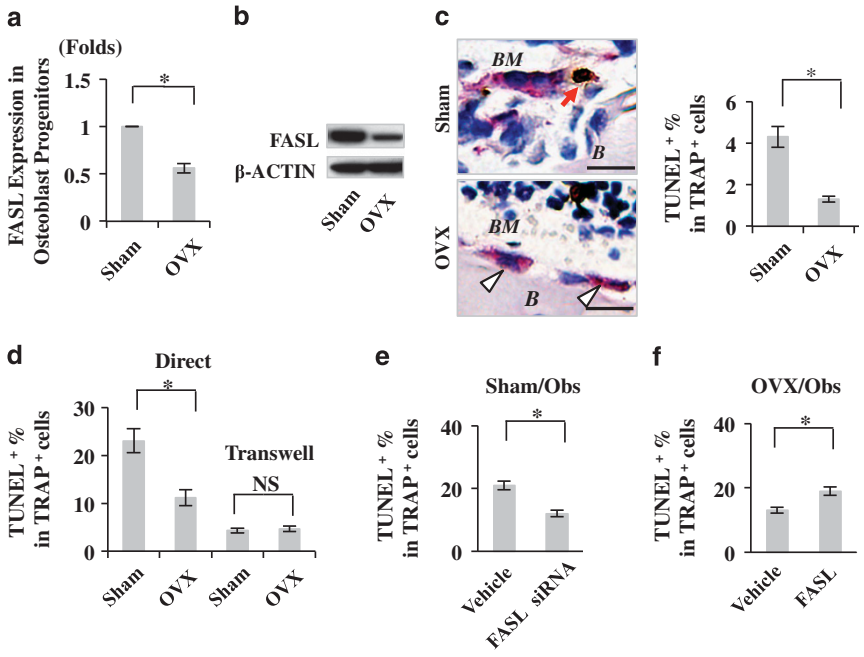

Figure 4 Reduced expression of FASL in OVX osteoblast progenitors. (**a** and **b**) PCR array and western blot showed that FASL was downregulated in OVX-derived osteoblast progenitors. (**c**) TUNEL-TRAP double staining showed that OVX mice presented a reduced number of apoptotic osteoclasts in femurs compared with the control group. (**d**) TUNEL-TRAP double staining showed that OVX-derived osteoblasts induced fewer apoptotic osteoclasts when compared with the control sham osteoblasts in the coculture system. (**e**) Knockdown of FASL expression in osteoblasts by siRNA resulted in reduced capacity to induce osteoclast apoptosis in the coculture system. (**f**) Overexpression of FASL in OVX-derived osteoblasts by lentivirus transfection rescued the capacity to induce osteoclast apoptosis in the coculture system. B, bone; BM, bone marrow; white triangles, $TRAP^+$ cells; red arrows, $TUNEL^+TRAP^+$ cells; error bars represent mean ± S.E.M., and all the experiments were performed in triplicate, $n = 8$ animals per group. $^*P < 0.05$. Scale bar, 100 μm

could not be controlled. It has been demonstrated that OVX results in elevation of RANKL, an important mediator of osteoclast differentiation.[33] Here we demonstrated that the OVX-induced increase of RANKL/OPG levels were comparable between FASL cKO mice and their wild-type littermates (Figures 6f and g), suggesting that RANKL/OPG are not the key factors to determine the different degrees of OVX-induced bone loss between FASL cKO mice and their wild-type littermates.

In summary, we revealed that under physiological condition, osteoblasts express FASL to induce apoptosis in mature osteoclasts, serving as an intrinsic mechanism to maintain bone mass (Supplementary Figure 9A). OVX induces FASL downregulation in osteoblast progenitors/osteoblasts through IFN-γ- and TNF-α-induced NFκB activation (Supplementary Figure 9B).

Discussion

Previous studies showed that several soluble factors, such as RANKL, OPG, TGF-β, EphrinB2, Sema4D and Sema3A, have important roles in regulating the interaction between osteoblasts and osteoclasts.[7–10,15,34–37] As osteoblast precursors/osteoblasts express membrane-bounded FASL and osteoclasts express FAS,[23,29] osteoblast–osteoclast contact is very likely to happen during the bone remodeling process. Thus, it is reasonable to assume that osteoblast lineage cells are capable of inducing osteoclast apoptosis to serve as an alternative mechanism to govern osteoclast activity. The FASL-mediated FAS death pathway has been extensively investigated in the interplay between immune cells, cancer cells and MSC-based immunomodulation.[18–20,28] Previous studies showed that reduced osteoclast apoptosis may contribute to osteoporotic phenotype and that estrogen could upregulate FASL expression in osteoblasts to induce increased osteoclast apoptosis.[21–24] However, the functional role of osteoblast-expressed FASL in the maintenance of bone mass under physiological and pathological conditions is unknown. In this study, we establish the functional role of osteoblast-expressed FASL in the maintenance of bone mass under both physiological and pathological conditions, and found that proinflammatory factors indeed have a critical role in inducing downregulation of FASL expression of the osteoblastic lineage cells in OVX mice.

We cocultured osteoblasts with matured osteoclasts, which had undergone differentiation after exposure to a high concentration of osteoclast differentiation factors, including RANKL and M-CSF.[10,12–16] We then used this coculture system to determine whether osteoblasts could induce apoptosis of matured osteoclasts. Indeed, we found that wild-type osteoblasts, but not FAS-null (*gld*) osteoblasts, could induce apoptosis of mature osteoclasts. To clarify the specific role of FASL in osteoblasts, we generated FASL cKO mice and found that the FASL cKO mice exhibited significant osteopenia phenotype as a result of decreased osteoclast apoptosis and increased osteoclast activity, but without alteration in the levels of RANKL and OPG. Osteoblast progenitors derived from FASL cKO mice bone marrow showed reduced capability to induce osteoclast apoptosis *in vitro*, consistent with the results obtained in the *in vitro* experiments using osteoblasts from

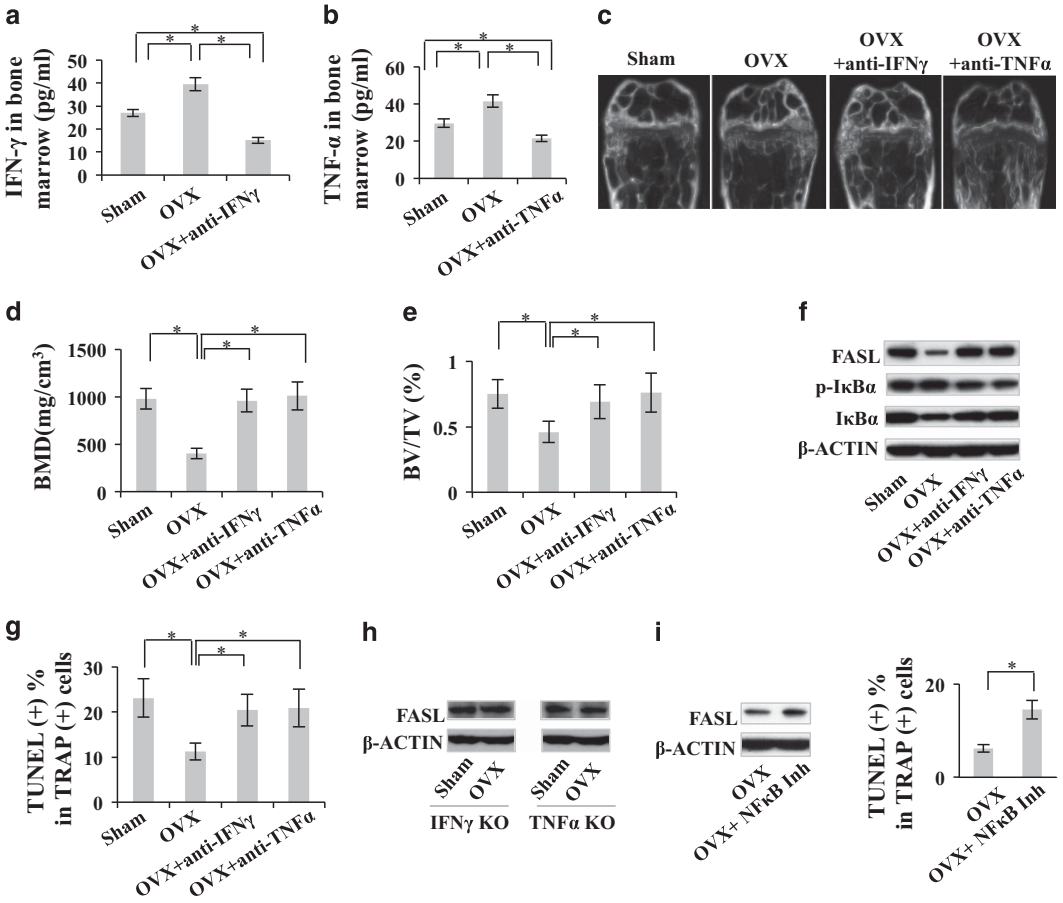

Figure 5 FASL deficiency in OVX-derived osteoblast progenitors is mediated by IFN-γ/TNF-α-induced NFκB activation. (**a** and **b**) ELISA showed that systemic injection of either IFN-γ or TNF-α neutralizing antibody into OVX mice was able to markedly decrease the levels of IFN-γ and TNF-α, respectively, in the bone marrow. (**c**–**e**) μCT showed that either IFN-γ or TNF-α neutralizing antibody could increase BMD and BV/TV of femurs. (**f**) Western blot showed that OVX-derived osteoblasts showed downregulation of FASL and upregulation of p-NFκB and p-IκB compared with those from sham control group, and either IFN-γ or TNF-α neutralizing antibody administration rescued the FASL expression with downregulation of p-IκB in the osteoblasts derived from OVX mice. (**g**) TUNEL-TRAP double staining showed that either IFN-γ or TNF-α neutralizing antibody administration restored their capacity to induce osteoclast apoptosis *in vitro*. (**h**) Western blot showed that OVX failed to induce FASL downregulation in osteoblast progenitors of either IFN-γ knockout or TNF-α knockout mice. (**i**) Western blot and TUNEL-TRAP double staining showed that NFκB inhibitor IKK Inhibitor VII could rescue FASL expression in OVX osteoblasts, as well as restore their ability to induce osteoclast apoptosis *in vitro*. White triangles, TRAP$^+$ cells; red arrows, TUNEL$^+$TRAP$^+$ cells; error bars represent mean $\pm$ S.E.M., $n=6$ animals per group. $^*P<0.05$. Scale bar, 100 μm

FASL-null (*gld*) mice. It has been demonstrated that osteoblasts provide an important stem cell niche for HSCs.[1–4] However, we failed to detect any abnormality in HSCs of FASL cKO mice, suggesting that osteoblast lineage cells do not use FASL to contribute to the stem cell niche of HSCs.

RANKL is one of the most well-established regulators governing osteoclast development and function.[11] In FASL cKO mice, the levels of RANKL and OPG do not change. Using RANKL neutralizing antibody, we demonstrate that FASL/FAS pathway is independent of RANKL pathway as another intrinsic mechanism for osteoblasts to control over osteoclasts. RANKL/OPG and FASL/FAS may have independent and distinctive roles in regulating osteoclast activity, in which the RANKL/OPG system mainly contributes to osteoclast recruitment and differentiation, whereas FASL/FAS pathway is to remove matured osteoclasts. Moreover, we found that FASL expression by osteoblast lineage cells was decreased during differentiation. Previous studies showed that the RANKL expression by osteoblast lineage cells is decreased during differentiation.[38,39] Thus, FASL and RANKL expressions in the osteoblast lineage cells are dependent on the stages of differentiation. The study by Park *et al*.[40] showed that FASL-mediated osteoclastogenesis of osteoclast progenitors. The different evidences found in the study by Park *et al*. and ours may be due to the fact that osteoclasts investigated in these two studies were at different differentiation stages. We showed that compared with osteoclast progenitors, mature osteoclasts presented higher FAS expression and showed much higher sensitivity to osteoblast-induced apoptosis. It is well demonstrated that osteoclastic lineage cells respond to RANKL-induced differentiation.[10] Therefore, at the stage of osteoclast progenitors, osteoclast lineage cells may preferentially undergo osteoclastogenesis via RANKL and FASL. However, at the stage of mature osteoclasts, osteoclast lineage cells may preferentially undergo osteoblast-induced apoptosis via FASL. Thus, it suggested that the differentiation stages of osteoclasts mediate the switch and coexist with osteoblast-induced osteoclast apoptosis and osteoclastogenesis.

Increasing evidence indicates that bone remodeling is under the control of factors related to immune regulation.[41]

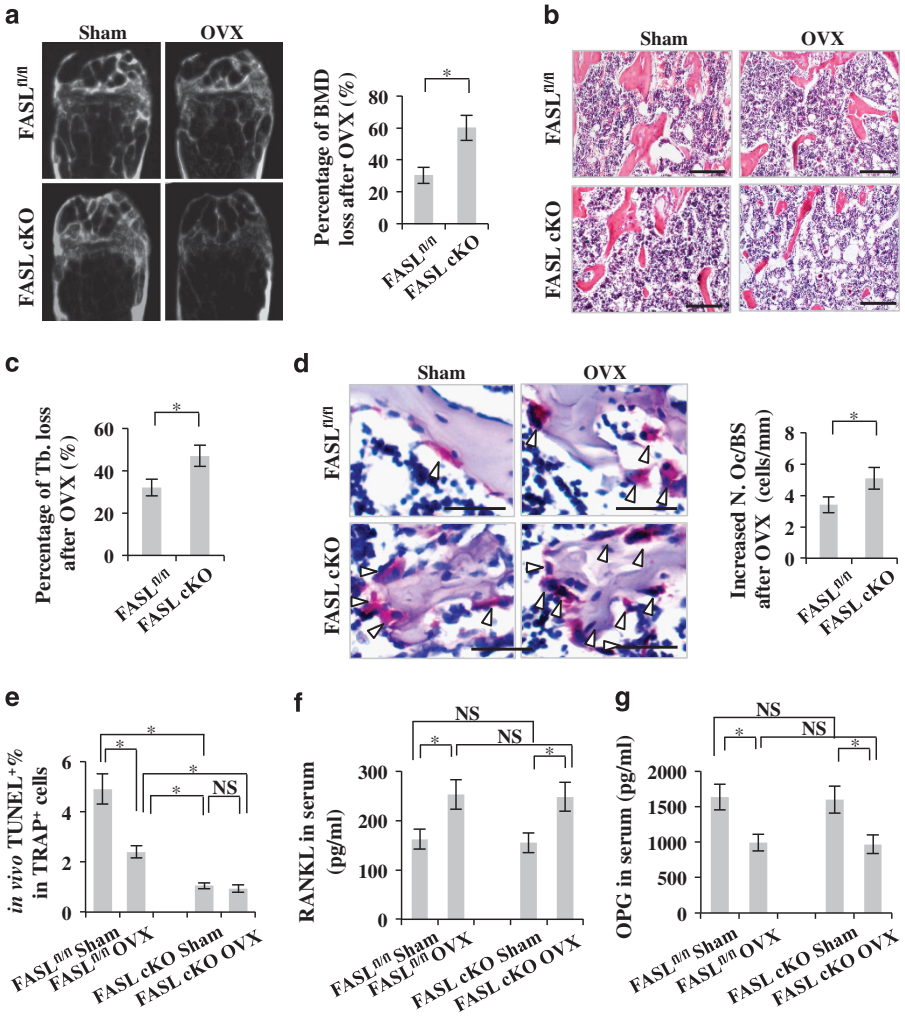

Figure 6 OVX induces more dramatic bone loss in FASL cKO mice. (**a**–**c**) μCT and HE staining showed that FASL cKO mice presented more dramatic decreases in bone mineral density and bone trabeculae percentage in the femurs when compared with their wild-type littermates. (**d**) TRAP staining showed that FASL cKO mice presented more dramatically elevated osteoclast activity when compared with their control littermates. (**e**) TUNEL-TRAP double staining showed that although OVX was able to induce decreased ratio of apoptotic osteoclasts in wild-type mice, FASL cKO mice presented the lowest ratio of apoptotic osteoclasts regardless of sham or OVX procedures. (**f** and **g**) ELISA showed that the OVX-induced increase of RANKL/OPG levels were comparable between FASL cKO mice and their wild-type littermates. Error bars represent mean ± S.E.M., $n = 6$ animals per group. $^*P < 0.05$. Scale bar, 100 μm

It is widely accepted that proinflammatory cytokines induce osteoclastogenesis[42–45] and that IFN-γ and TNF-α synergistically affect self-renewal and differentiation of osteoblast progenitors.[6] In this study, we demonstrate that long-term exposure to IFN-γ and TNF-α results in reduced expression of FASL in osteoblasts via activation of the NFκB pathway. It is possible that other factors, such as estrogen, could also contribute to the regulation of FASL expression in osteoblast lineage cells. Estrogen can directly upregulate FASL in osteoclasts and C-C chemokine receptor-2 (CCR2) in osteoclast progenitor cells, thus regulating osteoclastogenesis and the lifespan of mature osteoclasts.[21,46] Meanwhile, estrogen upregulates TGFβ and soluble FASL in osteoblasts, leading to the apoptosis of osteoclast progenitors and osteoclasts, respectively.[22,23]

Several treatment strategies have been developed for osteoporosis, including direct inhibition of osteoclasts or stimulation of osteoblast function, but with compromised efficacy and significant side effects.[47,48] Therefore, more appropriate treatments need to be developed to synchronously modify the interplay between osteoblasts and osteoclasts.[49,50] In this study, we found that regulation of pro-inflammation by IFN-γ and TNF-α neutralizing antibodies rescued the decreased FASL expression of the osteoblastic lineage cells and finally rescued the osteopenic phenotype in OVX mice, suggesting new therapeutic methods aiming at rescuing impaired bone homeostasis.

Materials and methods

Animals. C3H/HeJ, C57BL/6, B6Smn.C3-FASL*gld*/J (FASL-null mice), C3MRLFAS*lpr*/J (FAS-null mice), B6;129S-*Tnf*^{tm1Gkl}/J (TNF-α knockout mice), B6.129S7-*Ifng*^{tm1Ts}/J (IFN-γ knockout mice) and B6.Cg-Tg(Sp7-tTA,tetO-EGFP/cre) 1Amc/J (Sp7-Cre mice) were purchased from the Jackson Lab (Bar Harbor, ME, USA). Immunocompromised mice (Beige nude/nude XIDIII) were purchased from Harlan (Indianapolis, IN, USA). The C57BL/6 mice carrying the FASL gene bordered with two loxP sequences were generated as previously described.[25] Such FASL$^{fl/fl}$ mice have previously been used successfully to examine the role of FASL in

a variety of cell types, including those in T cells, B cells and myeloid cells.[26] To generate FASL cKO mice, we used Sp7-Cre mice, in which the Cre recombinase gene is knocked into the Sp7 locus and specifically expressed in osteoblastic lineage.[27] The FASL cKO mice and normal $FASL^{fl/fl}$ littermates were generated by mating $Sp7\text{-}Cre^{+/-}$ $FASL^{fl/+}$ male mice with $Sp7\text{-}Cre^{-/-}$ $FASL^{fl/fl}$ female mice. Mice were genotyped by PCR with primers amplifying the Sp7-Cre transgene (5′-GCG GTCTGGCAGTAAAAACTATC-3′ and 5′-GTGAAACAGCATTGCTGTCACTT-3′) and FASL generating 'floxed' and null allele products.[25] These animal experiments were performed under institutionally approved protocols for the use of animal research (University of Southern California #10941, 11141 and 11327).

Micro-CT scan, bone histology and histomorphometry. After being harvested and fixed in 4% paraformaldehyde (PFA), femurs were scanned by Inveon micro-CT system (Siemens AG, Munich, Germany), and cross-sectional volumetric BMD and BV/TV were measured at right femur mid-diaphysis. We performed all static and dynamic bone histomorphometry analyses on femurs of 8-week-old FASL cKO mice and their littermates according to standard protocols of the American Society for Bone and Mineral Research, as previously described.[6,9,15,51] Briefly, we sectioned paraffin-embedded tissues to a 5 μm thickness and stained the section with H&E. We performed von Kossa and Trichrome's stains on 5–7 μm undecalcified femur plastic sections after embedding in methyl methacrylate. For assessment of dynamic bone formation, the mice were injected with calcein 10 and 2 days, respectively, before sacrifice, according to standard labeling procedure.[52]

Detection of osteoclast apoptosis. Apoptotic osteoclasts in femurs and cultured cells were detected by TUNEL-TRAP double staining. Briefly, the femur sections and cultured cells underwent TUNEL staining using an Apoptag peroxidase *in situ* apoptosis detection kit (Millipore, Billerica, MA, USA) according to the manufacturer's instruction, followed by TRAP staining counterstained with Gill's Hematoxylin. For quantification of apoptotic osteoclasts, 10 representative images were analyzed by using NIH ImageJ software. The results were shown as the percentage of TUNEL-positive cells out of TRAP-positive cells per total bone area.

***In vivo* osteoclast activity assay.** A mouse calvarial osteolysis model was used to determine inductive bone resorption as previously described.[53] Briefly, 5×10^5 Titanium particles (Alfa Aesar, Ward Hill, MA, USA) in 40 μl PBS were implanted on the surface of parietal bones of FASL cKO mice, *gld* mice or their littermates. After 7 days, parietal bones were harvested and processed for X-ray analysis using Digital X-ray Specimen PRO System (Carestream Health, Inc., Upland, CA, USA). The extent of osteolysis in each bone was determined from the X-ray images by using NIH ImageJ software.

Isolation of mouse osteoblast progenitors and osteogenic differentiation assay. Mouse osteoblast progenitors were isolated from femurs and tibias and cultured. Detailed methods are described in the Supplementary Experimental Procedures. For *in vitro* osteogenesis assay, mouse osteoblast progenitors were cultured to confluence and changed to an osteo-inductive media containing 2 mM β-glycerophosphate (Sigma, St. Louis, MO, USA), 100 mM L-ascorbic acid 2-phosphate (Wako Pure Chemical Industries Ltd., Chuo-Ku, Japan) and 10 nM dexamethasone (Sigma). After 4 weeks of osteo-inductive culture, calcium deposits were detected by staining with 1% Alizarin Red (Sigma). The mineralized areas were quantified by using NIH ImageJ and were shown as a percentage of Alizarin Red-positive area over total area. For *in vivo* osteogenic assay, ~ 4.0×10^6 osteoblast progenitors were mixed with HA/TCP ceramic particles (40 mg, Zimmer Inc., Warsaw, IN, USA) as a carrier and subcutaneously implanted into the dorsal surface of 8–10-week-old immunocompromised mice. At 8 weeks post implantation, the implants were harvested, fixed in 4% PFA and then decalcified with 10% EDTA (pH 7.4). After paraffin embedding, 6 μm paraffin sections were stained with H&E and analyzed by an NIH ImageJ. Five fields were selected, and newly formed mineralized tissue area in each field was calculated and shown as a percentage to total tissue area.

Osteoclast formation and coculture of osteoblast progenitors/osteoblasts with osteoclasts. Bone marrow cells (BMCs) were collected by frequent injection of PBS throughout the entire marrow cavity of the tibiae and femora from 8-week-old mice, and 0.5×10^6 BMCs were suspended in αMEM (Invitrogen, Grand Island, NY, USA) containing 15% heat-inactivated FBS (Equitech-Bio, Kerrville, TX, USA), L-glutamine (Invitrogen), penicillin and streptomycin (Invitrogen) and 20 ng/ml M-CSF (R&D, Minneapolis, MN, USA) in a 24-well plate for 48 h. The adherent cells were then collected and cultured with 20 ng/ml M-CSF (R&D) and 50 ng ml^{-1} sRANKL (PeproTech, Rocky Hill, NJ, USA) for another 4 days. For coculture assay, 0.1×10^6 osteoblast progenitors/osteoblasts, with or without knockdown of FASL or NFκB pathway, in normal media containing M-CSF and sRANKL were seeded into each upper chamber of 0.4 μm Transwell (Costar, Tewksbury, MA, USA) or directly in each well of the 24-well plate containing osteoclasts for an additional 2 days, followed by fixation and staining for TRAP or TUNEL according to the manufacturers' protocols.

Overexpression and knockdown of FASL in osteoblast progenitors/osteoblasts. For overexpression of FASL, 293T cells for lentivirus production were plated in a 1-cm dish until 80% confluence. Plasmids were mixed in proper proportion with gene expression vectors (Addgene17620): psPAX (Addgene12260): pCMV-VSV-G (Addgene8454) = 5:3:2, were mixed in opti-MEM with LipofectamineLTX (Invitrogen) according to the protocol of the manufacturer. EGFP expression plasmid (Addgene17618) was used as control. The supernatant was collected 24 h and 48 h after transfection and filtered through 0.45μm filter to remove cell debris. For infection, the supernatant containing lentivirus was added into osteoblast progenitors/osteoblasts culture in the presence of 4 μg/ml polybrene and the transgenic FASL expression was validated by GFP observation. For knockdown of FASL expression in osteoblast progenitors/osteoblasts, siRNA transfection was used according to the manufacturer's instructions. Fluorescein-conjugated control siRNA was used as a control and as a method of evaluating transfection efficacy. All siRNA products were purchased from Santa Cruz Biotechnology (Dallas, TX, USA).

Western blot analysis. Twenty micrograms of protein were used, and SDS-PAGE and western blotting were performed according to standard procedures. β-Actin on the same membrane served as the loading control. Detailed procedures are described in Supplementary Experimental Procedures.

Flow cytometry analysis for osteoclast progenitors. A single-cell suspension of mouse bone marrow cells was stained with anti-CD3ε (eBioscience, San Diego, CA, USA), anti-B220 (eBioscience), anti-CD11b (eBioscience), anti-CD115 (eBioscience) and anti-CD117 (eBioscience) antibodies. Flow cytometric analysis was performed using FACS LSR II (BD Biosciences, San Jose, CA, USA).

Measurement of biomarkers in blood serum and cell culture supernatant. Mouse peripheral blood serum collected from retro-orbital venous plexus and osteoblast progenitors/osteoblasts culture supernatant were collected, and the levels of RANKL, OPG, IFN-γ and TNF-α were detected using ELISA kits (RANKL and OPG from R&D; IFN-γ and TNF-α from BioLegend, San Diego, CA, USA) according to their manufacturers' instructions.

***In vivo* treatment with RANKL neutralizing antibody.** Eight-week-old FASL cKO mice and normal $FASL^{fl/fl}$ littermates were administered intraperitoneally with 300 μg/mouse of anti-mouse RANKL mAb (IK22-5, kindly provided by Dr. Hideo Yagita, Juntendo University School of Medicine, Tokyo, Japan) or control rat IgG (Sigma) three times per week for 14 days, as previously described.[54] Two days after the last injection, bone analysis was performed as described earlier.

***In vivo* treatment with NFκB inhibitor IKK Inhibitor VII.** Six OVX mice and sham-operated ones were administered intraperitoneally with IKK Inhibitor XII or its isotype (Merck, Whitehouse Station, NJ, USA) at a concentration of 20 mg/kg three times per week for 14 days, as previously described. Two days after the last injection, bone analysis was performed as described above.

Ovariectomy-induced bone loss and administration of IFN-*γ* and TNF-*α* neutralizing antibodies. Generation of OVX mice in 12-week-old female mice was performed as described previously,[53] and age-matched mice receiving sham operation served as control. To deplete IFN-γ and TNF-α, at 1 day before OVX, mice were intraperitoneally injected with 250 μg of either IFN-γ or TNF-α neutralizing antibodies (BioLegend) in 0.5 ml sterile saline every 3 days until 21 days post OVX, respectively. In control groups, 250 μg isotype control antibodies in 0.5 ml sterile saline were identically administered. All mice were euthanized with CO_2 at day 28 after OVX and subjected to bone analysis as described earlier.

Induction of downregulated FASL in osteoblast progenitors by IFN-γ and TNF-α treatment. After seeding 0.5×10^6 osteoblast progenitors, with or without treatment using NFκB siRNA, onto each 6-well culture dish, IFN-γ (10 or 50 ng/ml) and TNF-α (5 ng/ml) in normal growth media were used to treat the osteoblast progenitors for 7 days, either separately or in combination. Total protein was extracted for detection of FASL and NFκB pathway markers using western blot.

Statistics. SPSS 13.0 (Armonk, NY, USA) was used to perform statistical analysis. Significance was assessed by independent two-tailed Student's *t*-test or ANOVA. The *P*-values <0.05 were considered significant.

Conflict of Interest

The authors declare no conflict of interest.

Acknowledgements. This work was supported by grants from the National Natural Science Foundation of China (No. 81020108019 to YJ and SS), from the National Basic Research Program (973 Program) of China (No. 2011CB964700 to YJ) and from National Institute of Dental and Craniofacial Research, National Institutes of Health, Department of Health and Human Services (R01DE017449 and R01DE019932 to SS).

Author contributions

LW, SL and YZ were involved in the practical achievement of the experiments. LW, SL, DL, YL and CC collected, analyzed and interpreted the data. LW and SL wrote the manuscript. SK provided some animals for the experiments. YJ and SS designed the study and provided financial and administrative support. All the authors read and approved the manuscript for publication.

1. Rankin EB, Wu C, Khatri R, Wilson TL, Andersen R, Araldi E *et al.* The HIF signaling pathway in osteoblasts directly modulates erythropoiesis through the production of EPO. *Cell* 2012; **149**: 63–74.
2. Calvi LM, Adams GB, Weibrecht KW, Weber JM, Olson DP, Knight MC *et al.* Osteoblastic cells regulate the haematopoietic stem cell niche. *Nature* 2003; **425**: 841–846.
3. Greenbaum A, Hsu YM, Day RB, Schuettpelz LG, Christopher MJ, Borgerding JN *et al.* CXCL12 in early mesenchymal progenitors is required for haematopoietic stem-cell maintenance. *Nature* 2013; **495**: 227–230.
4. Zhang J, Niu C, Ye L, Huang H, He X, Tong WG *et al.* Identification of the haematopoietic stem cell niche and control of the niche size. *Nature* 2003; **425**: 836–841.
5. Liu Y, Wang L, Kikuiri T, Akiyama K, Chen C, Xu X *et al.* Mesenchymal stem cell-based tissue regeneration is governed by recipient T lymphocytes via IFN-gamma and TNF-alpha. *Nat Med* 2011; **17**: 1594–1601.
6. Wang L, Zhao Y, Liu Y, Akiyama K, Chen C, Qu C *et al.* IFN-gamma and TNF-alpha synergistically induce mesenchymal stem cell impairment and tumorigenesis via NFkappaB signaling. *Stem Cells* 2013; **31**: 1383–1395.
7. Zhao C, Irie N, Takada Y, Shimoda K, Miyamoto T, Nishiwaki T *et al.* Bidirectional ephrinB2-EphB4 signaling controls bone homeostasis. *Cell Metab* 2006; **4**: 111–121.
8. Negishi-Koga T, Shinohara M, Komatsu N, Bito H, Kodama T, Friedel RH *et al.* Suppression of bone formation by osteoclastic expression of semaphorin 4D. *Nat Med* 2011; **17**: 1473–1480.
9. Hayashi M, Nakashima T, Taniguchi M, Kodama T, Kumanogoh A, Takayanagi H. Osteoprotection by semaphorin 3 A. *Nature* 2012; **485**: 69–74.
10. Lacey DL, Timms E, Tan HL, Kelley MJ, Dunstan CR, Burgess T *et al.* Osteoprotegerin ligand is a cytokine that regulates osteoclast differentiation and activation. *Cell* 1998; **93**: 165–176.
11. Wada T, Nakashima T, Hiroshi N, Penninger JM. RANKL-RANK signaling in osteoclastogenesis and bone disease. *Trends Mol Med* 2006; **12**: 17–25.
12. Franzoso G, Carlson L, Xing L, Poljak L, Shores EW, Brown KD *et al.* Requirement for NF-kappaB in osteoclast and B-cell development. *Genes Dev* 1997; **11**: 3482–3496.
13. Takayanagi H, Kim S, Koga T, Nishina H, Isshiki M, Yoshida H *et al.* Induction and activation of the transcription factor NFATc1 (NFAT2) integrate RANKL signaling in terminal differentiation of osteoclasts. *Dev Cell* 2002; **3**: 889–901.
14. Takayanagi H, Kim S, Matsuo K, Suzuki H, Suzuki T, Sato K *et al.* RANKL maintains bone homeostasis through c-Fos-dependent induction of interferon-beta. *Nature* 2002; **416**: 744–749.
15. Nakashima T, Hayashi M, Fukunaga T, Kurata K, Oh-Hora M, Feng JQ *et al.* Evidence for osteocyte regulation of bone homeostasis through RANKL expression. *Nat Med* 2011; **17**: 1231–1234.
16. Asagiri M, Sato K, Usami T, Ochi S, Nishina H, Yoshida H *et al.* Autoamplification of NFATc1 expression determines its essential role in bone homeostasis. *J Exp Med* 2005; **202**: 1261–1269.
17. Yasuda H, Shima N, Nakagawa N, Yamaguchi K, Kinosaki M, Mochizuki S *et al.* Osteoclast differentiation factor is a ligand for osteoprotegerin/osteoclastogenesis-inhibitory factor and is identical to TRANCE/RANKL. *Proc Natl Acad Sci USA* 1998; **95**: 3597–3602.
18. Hohlbaum AM, Moe S, Marshak-Rothstein A. Opposing effects of transmembrane and soluble FAS ligand expression on inflammation and tumor cell survival. *J Exp Med* 2000; **191**: 1209–1220.
19. Micheau O, Tschopp J. Induction of TNF receptor I-mediated apoptosis via two sequential signaling complexes. *Cell* 2003; **114**: 181–190.
20. Zhang Y, Xu G, Zhang L, Roberts AI, Shi Y. Th17 cells undergo FAS-mediated activation-induced cell death independent of IFN-gamma. *J Immunol* 2008; **181**: 190–196.
21. Nakamura T, Imai Y, Matsumoto T, Sato S, Takeuchi K, Igarashi K *et al.* Estrogen prevents bone loss via estrogen receptor alpha and induction of FAS ligand in osteoclasts. *Cell* 2007; **130**: 811–823.
22. Hughes DE, Dai A, Tiffee JC, Li HH, Mundy GR, Boyce BF. Estrogen promotes apoptosis of murine osteoclasts mediated by TGF-beta. *Nat Med* 1996; **2**: 1132–1136.
23. Krum SA, Miranda-Carboni GA, Hauschka PV, Carroll JS, Lane TF, Freedman LP *et al.* Estrogen protects bone by inducing FAS ligand in osteoblasts to regulate osteoclast survival. *EMBO J* 2008; **27**: 535–545.
24. Garcia AJ, Tom C, Guemes M, Polanco G, Mayorga ME, Wend K *et al.* ERalpha signaling regulates MMP3 expression to induce FASL cleavage and osteoclast apoptosis. *J Bone Miner Res* 2013; **28**: 283–290.
25. Karray S, Kress C, Cuvellier S, Hue-Beauvais C, Damotte D, Babinet C *et al.* Complete loss of FAS ligand gene causes massive lymphoproliferation and early death, indicating a residual activity of gld allele. *J Immunol* 2004; **172**: 2118–2125.
26. Mabrouk I, Buart S, Hasmim M, Michiels C, Connault E, Opolon P *et al.* Prevention of autoimmunity and control of recall response to exogenous antigen by FAS death receptor ligand expression on T cells. *Immunity* 2008; **29**: 922–933.
27. Rodda SJ, McMahon AP. Distinct roles for Hedgehog and canonical Wnt signaling in specification, differentiation and maintenance of osteoblast progenitors. *Development* 2006; **133**: 3231–3244.
28. Akiyama K, Chen C, Wang D, Xu X, Qu C, Yamaza T *et al.* Mesenchymal-stem-cell-induced immunoregulation involves FAS-ligand-/FAS-mediated T cell apoptosis. *Cell Stem Cell* 2012; **10**: 544–555.
29. Kovacic N, Grcevic D, Katavic V, Lukic IK, Grubisic V, Mihovilovic K *et al.* FAS receptor is required for estrogen deficiency-induced bone loss in mice. *Lab Invest* 2010; **90**: 402–413.
30. Jacquin C, Gran DE, Lee SK, Lorenzo JA, Aguila HL. Identification of multiple osteoclast precursor populations in murine bone marrow. *J Bone Miner Res* 2006; **21**: 67–77.
31. Yamaza T, Miura Y, Bi Y, Liu Y, Akiyama K, Sonoyama W *et al.* Pharmacologic stem cell based intervention as a new approach to osteoporosis treatment in rodents. *PLoS One* 2008; **3**: e2615.
32. Yamaza T, Ren G, Akiyama K, Chen C, Shi Y, Shi S. Mouse mandible contains distinctive mesenchymal stem cells. *J Dent Res* 2011; **90**: 317–324.
33. Kanematsu M, Sato T, Takai H, Watanabe K, Ikeda K, Yamada Y. Prostaglandin E2 induces expression of receptor activator of nuclear factor-kappa B ligand/osteoprotegrin ligand on pre-B cells: implications for accelerated osteoclastogenesis in estrogen deficiency. *J Bone Miner Res* 2000; **15**: 1321–1329.
34. Takayanagi H. Osteoimmunology: shared mechanisms and crosstalk between the immune and bone systems. *Nat Rev Immunol* 2007; **7**: 292–304.
35. Tang Y, Wu X, Lei W, Pang L, Wan C, Shi Z *et al.* TGF-beta1-induced migration of bone mesenchymal stem cells couples bone resorption with formation. *Nat Med* 2009; **15**: 757–765.
36. Xiong J, Onal M, Jilka RL, Weinstein RS, Manolagas SC, O'Brien CA. Matrix-embedded cells control osteoclast formation. *Nat Med* 2011; **17**: 1235–1241.
37. Wu X, Pang L, Lei W, Lu W, Li J, Li Z *et al.* Inhibition of Sca-1-positive skeletal stem cell recruitment by alendronate blunts the anabolic effects of parathyroid hormone on bone remodeling. *Cell Stem Cell* 2010; **7**: 571–580.
38. Atkins GJ, Kostakis P, Pan B, Farrugia A, Gronthos S, Evdokiou A *et al.* RANKL expression is related to the differentiation state of human osteoblasts. *J Bone Miner Res* 2003; **18**: 1088–1098.
39. Gori F, Hofbauer LC, Dunstan CR, Spelsberg TC, Khosla S, Riggs BL. The expression of osteoprotegerin and RANK ligand and the support of osteoclast formation by stromal-osteoblast lineage cells is developmentally regulated. *Endocrinology* 2000; **141**: 4768–4776.
40. Park H, Jung YK, Park OJ, Lee YJ, Choi JY, Choi Y. Interaction of Fas ligand and Fas expressed on osteoclast precursors increases osteoclastogenesis. *J Immunol* 2005; **175**: 7193–7201.
41. Nakashima T, Takayanagi H. Osteoimmunology: crosstalk between the immune and bone systems. *J Clin Immunol* 2009; **29**: 555–567.
42. Cenci S, Weitzmann MN, Roggia C, Namba N, Novack D, Woodring J *et al.* Estrogen deficiency induces bone loss by enhancing T-cell production of TNF-alpha. *J Clin Invest* 2000; **106**: 1229–1237.
43. Gao Y, Grassi F, Ryan MR, Terauchi M, Page K, Yang X *et al.* IFN-gamma stimulates osteoclast formation and bone loss *in vivo* via antigen-driven T cell activation. *J Clin Invest* 2007; **117**: 122–132.
44. Cenci S, Toraldo G, Weitzmann MN, Roggia C, Gao Y, Qian WP *et al.* Estrogen deficiency induces bone loss by increasing T cell proliferation and lifespan through IFN-gamma-induced class II transactivator. *Proc Natl Acad Sci USA* 2003; **100**: 10405–10410.

45. Roggia C, Gao Y, Cenci S, Weitzmann MN, Toraldo G, Isaia G *et al.* Up-regulation of TNF-producing T cells in the bone marrow: a key mechanism by which estrogen deficiency induces bone loss *in vivo*. *Proc Natl Acad Sci USA* 2001; **98**: 13960–13965.
46. Binder NB, Niederreiter B, Hoffmann O, Stange R, Pap T, Stulnig TM *et al.* Estrogen-dependent and C-C chemokine receptor-2-dependent pathways determine osteoclast behavior in osteoporosis. *Nat Med* 2009; **15**: 417–424.
47. Rachner TD, Khosla S, Hofbauer LC. Osteoporosis: now and the future. *Lancet* 2011; **377**: 1276–1287.
48. Lewiecki EM. New targets for intervention in the treatment of postmenopausal osteoporosis. *Nat Rev Rheumatol* 2011; **7**: 631–638.
49. Kikuiri T, Kim I, Yamaza T, Akiyama K, Zhang Q, Li Y *et al.* Cell-based immunotherapy with mesenchymal stem cells cures bisphosphonate-related osteonecrosis of the jaw-like disease in mice. *J Bone Miner Res* 2010; **25**: 1668–1679.
50. Favus MJ. Bisphosphonates for osteoporosis. *N Engl J Med* 2010; **363**: 2027–2035.
51. Parfitt AM, Drezner MK, Glorieux FH, Kanis JA, Malluche H, Meunier PJ *et al.* Bone histomorphometry: standardization of nomenclature, symbols, and units. Report of the ASBMR Histomorphometry Nomenclature Committee. *J Bone Miner Res* 1987; **2**: 595–610.
52. Vignery A, Baron R. Dynamic histomorphometry of alveolar bone remodeling in the adult rat. *Anat Rec* 1980; **196**: 191–200.
53. Miura M, Chen XD, Allen MR, Bi Y, Gronthos S, Seo BM *et al.* A crucial role of caspase-3 in osteogenic differentiation of bone marrow stromal stem cells. *J Clin Invest* 2004; **114**: 1704–1713.
54. Kamijo S, Nakajima A, Ikeda K, Aoki K, Ohya K, Akiba H *et al.* Amelioration of bone loss in collagen-induced arthritis by neutralizing anti-RANKL monoclonal antibody. *Biochem Biophys Res Commun* 2006; **347**: 124–132.

Supplementary Information accompanies this paper on Cell Death and Differentiation website (http://www.nature.com/cdd)